



## The layered $\text{Bi}_2\text{WO}_6$ phase: role of elaboration conditions on structure and luminescence properties

A. Taoufyq<sup>1,2,3,4,\*</sup>, H. Ait Ahsaine<sup>2</sup>, L. Patout<sup>1</sup>, A. Benlhachemi<sup>2</sup>, B. Bakiz<sup>2</sup>, M. Ezahri<sup>2</sup>, F. Guinneton<sup>1</sup>, A. Lyoussi<sup>3</sup>, G. Nolibe<sup>4</sup>, J-R Gavarri<sup>1</sup>,

<sup>1</sup> Institut Matériaux Microélectronique et Nanosciences de Provence, IM2NP, UMR CNRS 7334, Université de Toulon, BP 20132, 83957, La Garde Cedex, France.

<sup>2</sup> Laboratoire Matériaux et Environnement LME, Faculté des Sciences, Université Ibn Zohr, BP 8106, Cité Dakhla,

<sup>3</sup> Département d'Études des Réacteurs, Laboratoire Dosimétrie Capteurs Instrumentation, CEA, 13108, Cadarache, France.

<sup>4</sup> Société CESIGMA- signals & systems, 1576 Chemin de La Planquette, 83130, La Garde, France.

Received 8 September, Revised 10 October 2014, Accepted 19 October 2014

\*Corresponding Author. E-mail: [taoufyq@univ-tln.fr](mailto:taoufyq@univ-tln.fr); Tel: (+33 494 142 309)

### Abstract

In the present work, we investigate the structural and luminescence properties of the bismuth tungstate  $\text{Bi}_2\text{WO}_6$ . This phase is interesting because of its electrical [1], photocatalytic [2] and luminescence [3] properties. Polycrystalline samples were elaborated using a coprecipitation technique followed by a calcination process at different temperatures (300, 400, 600 and 900°C). The samples were characterized by X-ray diffraction, scanning and transmission electron microscopy (SEM, TEM) analyses. The space group  $\text{Pca}_2_1$  has been confirmed for this phase. The transmission electron microscopy analysis showed that this structural configuration is valid at a very low scale. Crystal cell parameters and cell volume depend on elaboration temperature. Luminescence experiments of these polycrystalline samples were performed under UV-laser light irradiation. Luminescence intensities depend on the elaboration conditions.

**Keywords:** Bismuth tungstate, co-precipitation method, Microstructural study, luminescence properties.

### Introduction

Currently, Many ecological problems linked with a radiation safety of man, environmental control, individual dosimetry, nuclear medicine and X-ray computer tomography, together with scientific and technical problems of radiation monitoring in the case of different nuclear facilities for the fundamental and applied physics, are all related to the development of reliable methods for detection of ionizing radiation. Hence, we need to develop new material scintillators, more sensitive and selective to detect these hazardous radiations. Semiconductors are of enormous technological importance because of their special properties. In fact, they are used in many fields such as photoluminescence [4], solar-cells [5-6], microwave applications [7], optical fiber scintillator material [8], gas sensors and catalysis [9]. One of these semiconductors is the bismuth tungstate  $\text{Bi}_2\text{WO}_6$ . This latter is a typical multifunctional material presenting several properties: luminescence under UV or X-ray excitation [3], photocatalytic activity [2] piezoelectricity and ionic conduction [1]; recently we have studied the electrical conductivity and showed that this phase showed a major ion conduction at high temperature.

The bismuth tungstates were previously synthesized by coprecipitation method [1], solid-state reaction [10] between  $\text{Bi}_2\text{O}_3$  and  $\text{WO}_3$  stoichiometric mixtures, sol-gel method [11], combustion synthesis method [12], ultrasonic method and hydro/solvo-thermal method [8]. This phase is a layered compound with alternating  $\text{Bi}_2\text{O}_2^{2+}$  and  $\text{WO}_4^{2-}$  layers: its structure was determined with a space group  $\text{Pca}_2_1$  [1].

In the study, we investigate the structural and luminescence properties of the bismuth tungstate  $\text{Bi}_2\text{WO}_6$ .

We have prepared polycrystalline  $\text{Bi}_2\text{WO}_6$  materials from a specific coprecipitation method followed by thermal treatment. The obtained material was characterized using X-ray diffraction (XRD), Scanning and

Transmission Electron Microscopy (SEM, TEM). Finally, we have performed luminescence properties of these polycrystalline samples under UV-laser irradiation.

## 2. Materials and methods

### 2.1. Synthesis

Samples of bismuth tungstate phase  $\text{Bi}_2\text{WO}_6$  were produced using the coprecipitation method previously described by Obregón Alfaro et al. [1, 13]. The preliminary precursors were bismuth nitrate and ammonium tungstate in aqueous solutions. The pentahydrate Bismuth (III) nitrate  $\text{Bi}(\text{NO}_3)_3 \cdot 5\text{H}_2\text{O}$  [Alfa aesar, no. 10657 (99.9%)] was dissolved in a volume of diluted  $\text{HNO}_3$  (10%, v/v) at  $25^\circ\text{C}$ . This nitrate solution was slowly added to 0.1 L of an aqueous solution of  $(\text{NH}_4)_{10}(\text{W}_{12}\text{O}_{41}) \cdot 6\text{H}_2\text{O}$  [Alfa aesar, no. 22640 (99.9%)] under vigorous stirring. Ammonium hydroxide ( $\text{NH}_4\text{OH}$ ) was added to the solution in order to adjust the pH (pH = 5). The mixture was stirred and kept in a water bath around  $70$  to  $80^\circ\text{C}$ , in order to obtain a slow evaporation of water until the formation of a white solid, which was used as final precursor. Finally, this precursor powder was thermally treated at  $300$ ,  $600$  and  $900^\circ\text{C}$ , in air for 4 hours.

### 2.2. Characterization techniques

**X-ray diffraction.** The polycrystalline samples were analyzed by X-ray diffraction (XRD), using the EMPYREAN Panalytical diffractometer, equipped with a copper X-ray source (wavelength  $\lambda = 1.54 \cdot 10^{-10}$  m, tension  $V = 45$  kV, intensity  $I = 35$  mA), and with a Ni filter eliminating the  $K_\beta$  radiation. The diffractometer was equipped with a Pixel-1D-Detector. The XRD analysis was carried out using the classical  $\theta$ - $2\theta$  configuration, in continuous mode, with a step size of  $0.0016413$ , a scan speed of  $0.002$   $^\circ/\text{s}$ . All samples were powders compacted in a specific sample holder. The average crystallite's size of the prepared powders was evaluated from the half-widths of diffraction peaks using the Scherrer formula [15-17]

$$D = \frac{K \cdot \lambda}{\beta \cdot \cos(\theta)}$$

where  $\lambda$  is the wavelength of X-ray ( $\lambda_{\text{CuK}\alpha 1} = 1.54 \times 10^{-10}$  m);  $K$  is a Scherrer constant ( $K = 0.9$  in this case);  $\theta$  is the diffraction angle associated with a Bragg peak;  $\Delta 2\theta = (\Delta 2\theta_m^2 - \Delta 2\theta_s^2)^{1/2}$  is the corrected full width at half maximum (FWHM),  $\Delta 2\theta_m$  being the total FWHM of the Bragg peak,  $\Delta 2\theta_s$  being that of a standard crystallized sample of  $\text{Bi}_2\text{WO}_6$ .

**Microstructural techniques.** Scanning and transmission electron microscopy (SEM, TEM) analyses were used to observe the nanoparticle morphology. Preliminary images were obtained with a SUPRA 40 VP COLONNE GEMINI ZEISS SEM using a maximum voltage of  $20$  kV. TEM analyses were carried out using a Tecnai G2 microscope operating at  $200$  kV with a  $\text{LaB}_6$  filament. The objective of these TEM analyses, including high-resolution imaging, was to study the structure at the local level.

**Luminescence.** The equipment used to perform the measurements of luminescence under UV was the previously described spectrometer Horiba Jobin-Yvon HR800 LabRam. The entrance slit, positioned behind the filter, is a diaphragm whose diameter can range from  $1$  to  $200$   $\mu\text{m}$ . The irradiated zone was limited to  $1$   $\mu\text{m}$  in diameter for all samples. The spherical mirror characterized by a  $800$  mm focal length allows reflecting the scattered radiation from the input to the dispersive grating to obtain spectra slot. The  $364.5$  nm line of an Ar-ion laser was used as the excitation source. The power applied to the samples was fixed to  $0.005$  mW with an acquisition time set to  $100$  milliseconds.

## 3. Results and discussion

### 3.1. X-ray diffraction analyses

Two complementary softwares were used to determine the cell parameters and determine the structure: the first one was a classical program calculating the cell parameters from Bragg peak positions, based on least square method, and the second one was the FULLPROF software using the Rietveld method [14]. The refinement results were obtained using the space group  $\text{Pca}2_1$ . The observed and calculated profiles of the sample treated at  $900^\circ\text{C}$  are shown in Figure 1. The difference curve shows a good agreement between the observed and calculated patterns. The structural study as a function of heat treatment temperature indicates an evolution of the full width at half maximum of the diffraction peaks and the lattice parameters ( $a$ ,  $b$ ,  $c$ ) and the cell volumes.

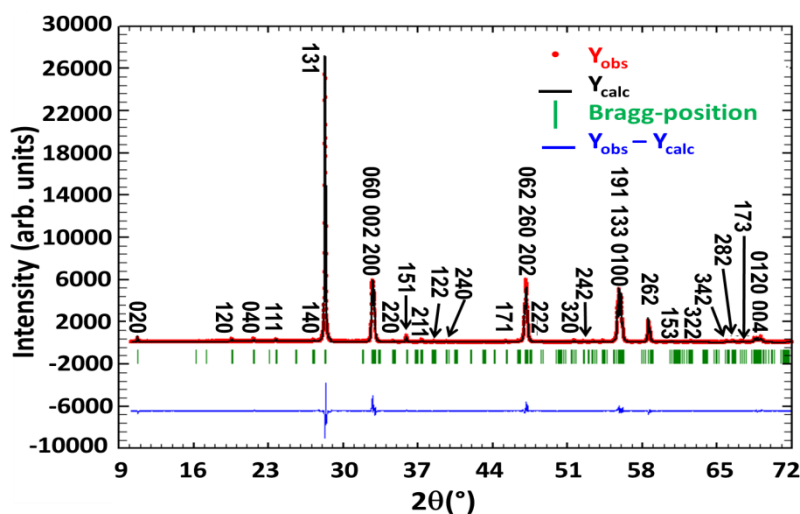


**Figure 1:** Calculated and observed diffraction profiles from Rietveld analysis for the  $\text{Bi}_2\text{WO}_6$  phase (space group  $\text{Pca}2_1$ ), thermally treated at  $900^\circ\text{C}$ .

Table 1 gives the values of the crystal cell parameters as a function of the thermal treatment: lattice parameters and cell volumes. In this Table, we have reported the linear dimensions of crystallites (D) determined from the Scherrer approach [15].

**Table 1:** lattice parameters, cell volumes and crystallite sizes as a function of the thermal treatment

	BWO-300°C	BWO-400°C	BWO-600°C	BWO-900°C
<b>a(Å)</b>	5.39(3)	5.41(3)	5.433(4)	5.434(3)
<b>b(Å)</b>	16.27(6)	16.34(9)	16.41(1)	16.424(8)
<b>c(Å)</b>	5.41(6)	5.46(2)	5.457(5)	5.456(4)
<b>V(Å<sup>3</sup>)</b>	475 (3)	482(4)	486.7(7)	487.0(5)
<b>D (nm)</b>	14(3)	17(4)	35(6)	136(25)

### 3.2. Microstructural study

The scanning electron analyses (Figure 2) show that the as prepared powder is constituted of a bimodal distribution of small and large grains (dimensions ranging between 0.1 and  $5\ \mu\text{m}$ ). The surface of large grains presents a granular aspect with smaller grains having dimensions of 20 to 50 nm. The EDX local microanalysis is congruent with the chemical composition of  $\text{Bi}_2\text{WO}_6$  with presence of gold due to the metallization for SEM analysis. The ratio Bi/W is constant.

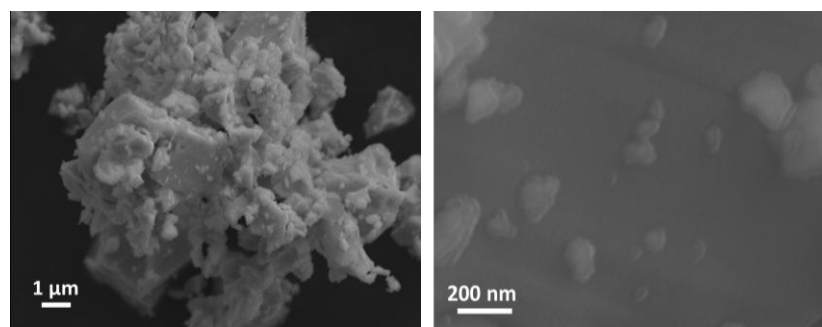


**Figure 2:** Scanning electron microscopy analysis of the  $\text{Bi}_2\text{WO}_6$  phase thermally treated at  $900^\circ\text{C}$ .

The main objective of these experiments was to confirm (or not) the space group and the disordered nature of this phase at the local scale. The electron diffraction patterns of highest symmetry axes (figure 3(a, b and c)) allowed confirming the orthorhombic crystal system and the unit cell parameters. The microdiffraction pattern corresponding to [010] zone axis confirmed the existence of a primitive Bravais lattice and of a-type glide planes. The [uv0] tilted series (figure 3 (d, e and f)) showed the presence of  $2_1$  helicoidal axes. Consequently, only three space groups can be associated with these symmetry elements (P,  $2_1$ , a):  $Pca2_1$ ,  $Pmn2_1$  and  $Pna2_1$ . In the [010] or [100] zone axes patterns, we observe extinctions only along the  $a^*$  or  $c^*$  directions respectively, which excludes the presence of any n-type glide plane. Consequently, the sole space group compatible with our data at a local scale is the  $Pca2_1$  one.

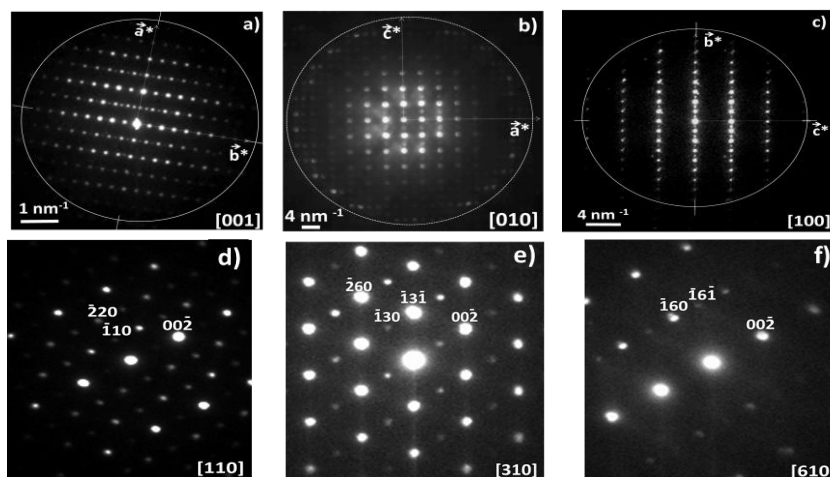


**Figure 3:** Electron diffraction pattern of highest symmetry and tilted [uv0] tilted for single crystal  $Bi_2WO_6$

### 3.3. Luminescence properties

The UV-laser light luminescence spectra obtained under excitation with an UV source (364.5 nm) are presented in Figure 4. The emission spectra were specified using Gaussian analysis in combination with the Labspec program. The luminescence is characterized by a broad spectral band covering the 350-700 nm range and has a maximum of 550 nm (2.2 eV).

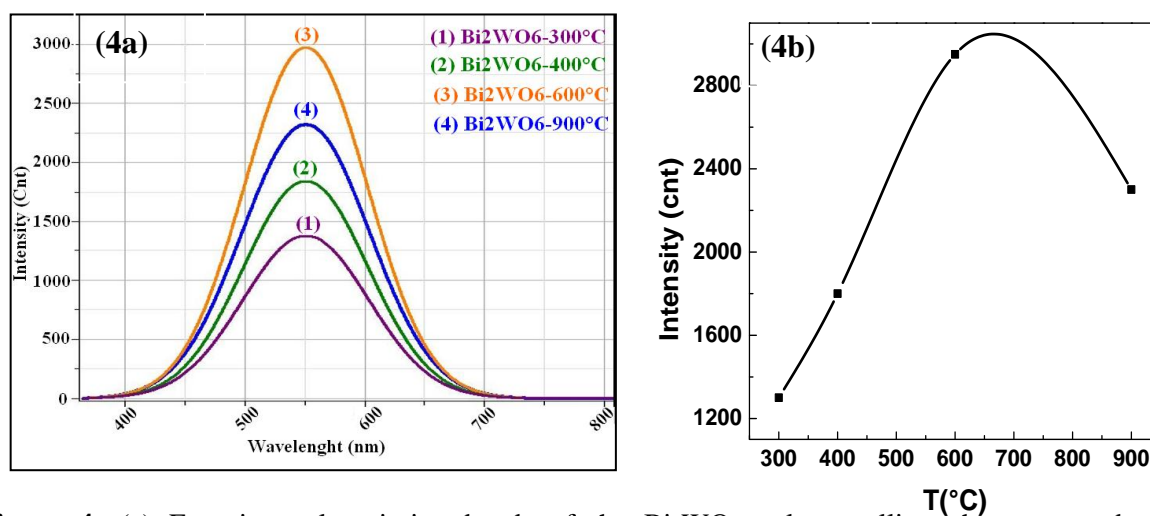


**Figure 4:** (a) Experimental emission bands of the  $Bi_2WO_6$  polycrystalline phases treated at different temperatures luminescence under UV excitation (364.5nm), (b) Variation of intensity with elaboration temperature.

In relation to temperature, it can be clearly noticed that the maximum luminescence intensity was obtained for the sample heated at 600 °C. In their study [16], the authors noted that the maximum luminescence intensity was reached for samples having intermediate defect amounts due to diversified thermal treatments: they considered that luminescence should be maximal for samples being neither excessively ordered nor excessively disordered. The best luminescence emission is obtained for the structure (600°C) that is neither highly disordered (300 and 400°C) nor highly ordered (900°C). Calcinations at higher temperatures would lead to a further increase in the short and long range order, and photoluminescence emission would not occur.

## Conclusion

In this study, we have synthesized the pure Bi<sub>2</sub>WO<sub>6</sub> phase from a coprecipitation technique followed by a calcination process at different temperatures (300, 400, 600 and 900°C). The space group Pca2<sub>1</sub> has been confirmed for this phase. The transmission electron microscopy analysis showed that this structural configuration is valid at a very low scale. We have observed a continuous variation of cell parameters with an increasing volume as the crystal sizes D increase. The luminescence analyses under UV excitation show that the elaboration conditions have a strong influence on the emission intensity. This might be due to coupling of structural defects and crystallite size effect, in the Bi<sub>2</sub>WO<sub>6</sub> structure.

## Acknowledgements

This work was financially supported by the Regional Council of Provence-Alpes - Côte d'Azur, the European Funds for Regional Development, the General Council of Var and by Toulon Provence Mediterranean, in the general framework of NANOGAMMA project (Grant number : 2010-16028/42169 ; collaboration between IM2NP, CEA of Cadarache, CESIGMA and IBS Societies) and international ARCUS-CERES project. This study was also developed in the general framework of CNRS-CNRST project (2014).

## References

1. Taoufyq A., Ait Ahsaine H., Patout L., Benlhachemi A., Ezahri M., Guinneton F., Lyoussi A., Nolibé G., Gavarrí J.-R., *J. Solid State Chem.* 203 (2013) 8-18.
2. Dumrongrojthanath P., Thongtem T., Phuruangrat A., Thongtem S., *J. Superlattice Microst.* 54 (2013) 71-77.
3. Bordun O.M., Kukharskii I.I., *J. Appl. Spectrosc.* 69 (4) (2002) 639-641.
4. Mikhailik V.B., Kraus H., Wahl D., Itoh M., Koike M., Bailiff I. K., *J. Phys. Rev. B*, 69 (20) (2004) 205110-205110-9.
5. Djouadi D., Chelouche A., Aksas A., *J. Mater. Environ. Sci.* 3 (3) (2012) 585-590.
6. Sadki H., Bennani M.N., Hamidi M., Bouachrine M., *J. Mater. Environ. Sci.* 5 (S1) (2014) 2156-2162.
7. Sczancoski J.C., Cavalcante L.S., Joya M.R., Varela J.A., Pizani P.S., Longo E., *J. Chem. Eng.* 140 (2008) 632-637.
8. Nikl M., Bohacek P., Mihokova E., Kobayashi M., Ishii M., Usuki Y., Babin V., Stolovich A., Zazubovich, Bacci M., *J. Lumin.* 87-89 (2000) 1136-1139.
- 9- Abderrahim H., Berrebia M., Hamou A., Kherief H., Zanon Y., Zenata K., *J. Mater. Environ. Sci.* 2 (2) (2011) 94-103.
10. 5. Finlayson A.P., Ward E., Tsaneva V.N., Glowacki B.A., *J. Power Sources* 145 (2005) 667-674.
11. Zhang G.K., Lü F., Li M., Yang J.L., Zhang X.Y., Huang B.B., *J. Phys. Chem. Solids* 71 (2010) 579-582.
12. Zhang Z., Wang W., Shang M., Yin W., *J. Hazard. Mater.* 177 (2010) 1013-1018.
13. Obregón Alfaro S., Martínez-de la Cruz A., *J. Appl. Catal. A* 383 (2010) 128-133.
14. Roisnel T., Rodríguez-Carvajal J., Delhez R., Mittenmeijer E.J., *Proceedings of the Seventh European Powder Diffraction Conference Spain* (2000) 118-123.
15. Pullar R.C., Taylor M.D., Bhattacharya A.K., *J. Eur. Ceram. Soc.* 18 (1988) 1759-1764.
16. Pôrto S.L., Longo E., Pizani P.S., Boschi T.M., Simões L.G.P., Lima S.J.G., Ferreira J.M., Soledade L.E.B., Espinoza J.W.M., Cassia-Santos M.R., Maurera M.A.M.A., Paskocimas C.A., Santo I.M.G., Souza A.G., *J. Solid State Chem.* 181(2008)1876-1881.

(2014) ; <http://www.jmaterenvironsci.com>